Lasers in Surgery and Medicine 24:236–243 (1999)

Simultaneous Irradiation and Imaging of Blood Vessels During Pulsed Laser Delivery

Jennifer Kehlet Barton, PhD,[1]* Daniel X. Hammer, MS,[2] T. Joshua Pfefer, MS,[2] David J. Lund, BS,[3] Bruce E. Stuck, MS,[3] and A.J. Welch, PhD[2]

[1]Biomedical Engineering Program, University of Arizona, Tucson, Arizona 85721
[2]Biomedical Engineering Program, The University of Texas at Austin, Austin, Texas 78712
[3]U.S. Army Medical Research Detachment of the Walter Reed Army Institute of Research, Armstrong, Brooks Air Force Base, San Antonio, Texas 78235

Background and Objective: **Simultaneous irradiation and viewing of 10–120 μm cutaneous blood vessels were performed to investigate the effects of 2-μs 577-nm dye laser pulses.**
Study Design/Materials and Methods: **A modified scanning laser confocal microscope recorded vessel response to different radiant exposures (J/cm^2). Probit analysis determined the 50% probability ("threshold") radiant exposure necessary to cause embolized or partly occluding coagula, coagula causing complete blood flow stoppage, and hemorrhage.**
Results: **A statistically significant difference in the threshold radiant exposure existed for each damage category for blood vessels 10–30 μm in diameter, but not for larger vessels. For vessels over 60 μm, complete flow stoppage was unattainable; increasing laser pulse energy produced hemorrhage. In larger vessels, coagula often were attached to the superficial vessel wall while blood flowed underneath. Monte Carlo optical and finite difference thermal modeling confirmed experimental results.**
Conclusion: **These results provide insight into the role of pulse duration and vessel diameter in the outcome of pulsed dye laser irradiation. Lasers Surg. Med. 24:236–243, 1999.**
© 1999 Wiley-Liss, Inc.

Key words: confocal microscopy; pulsed dye laser; finite difference model; Monte Carlo model; port wine stains

INTRODUCTION

Previous studies examining the effect of laser irradiation on cutaneous blood vessels have generally relied on surface information or stained histology sections obtained from biopsies. Surface information provided real-time but only indirect evidence of events that occurred in the blood vessel plexus, whereas stained histology sections provided detailed documentation of laser effects but was limited in temporal information. The present study was undertaken to achieve simultaneous micron-scale viewing and laser irradiation of cutaneous blood vessels. We examined the effects of a 577-nm 2-μs pulsed dye laser on 10–120-μm-diameter blood vessels in a hamster dorsal skin flap preparation. The short pulse duration illustrated an extreme; energy was deposited quickly

Contract grant sponsor: Office of Naval Research Free Electron Laser Biomedical Science Program; Contract grant number: N00014-91-J-1564; Contract grant sponsor: Albert and Clemmie Caster Foundation.

*Correspondence to: Jennifer K. Barton, University of Arizona, ECE Building 104, Tucson, AZ 85721-0104.
E-mail: barton@u.arizona.edu

Accepted 23 October 1998

© 1999 Wiley-Liss, Inc.

into a highly absorbing media before any significant heat conduction occurred.

Previous investigations have shown that microsecond pulsed dye lasers operating at 577 nm cause highly specific damage to cutaneous blood vessels [1–3] but are ineffective in treating port-wine stains (PWS) [4]. A proposed explanation is that the short pulse duration prevents sufficient transfer of heat from the absorber (oxyhemoglobin in the erythrocytes) to the vessel wall to coagulate and destroy the vessels. Immediate histology in these studies, which used 0.3–2.0-μs pulses, uniformly showed clusters of aggregated erythrocytes, endothelial damage including vessel rupture, and extravasation of erythrocytes. After 48 hr, necrosis of the vessel wall was seen in some cases [1], but endothelial regeneration dominated [1,4]. Tearing (rather than coagulating) the vessel wall appeared to be insufficient to destroy blood vessels. Clinical studies have also shown that 585-nm laser irradiation frequently achieves a superior clinical outcome than does 577-nm irradiation in the treatment of PWS [5]. Analytical investigations have indicated that this improvement may be due to the increased penetration of 585 nm light in blood, leading to more uniform heating and coagulation of blood vessels [6–8]. This effect should be more pronounced for large blood vessels (diameter > 577-nm penetration depth in blood of ~30 μm).

The overall objectives of this study were to advance technology (both measurement and analysis) and to examine the process of vessel coagulation. Experiments were performed to view directly the mechanism of microsecond-pulse 577-nm laser–blood vessel interaction and to determine whether coagulation of blood vessels was a function of vessel diameter. Irradiated blood vessels were examined for evidence of uneven or incomplete damage. A novel optical–thermal analysis tool was employed to predict the results of laser irradiation and provide insight into experimental observations.

MATERIALS AND METHODS

Five 120-g Syrian Golden hamsters were implanted with dorsal skin flap window preparations. The preparation provided an in vivo model for examining directly the effects of laser irradiation on blood vessels [9]. The subdermal blood vessels, which traversed an approximately 100-μm-thick layer of connective tissue, were exposed for observation, but a full thickness of normal skin

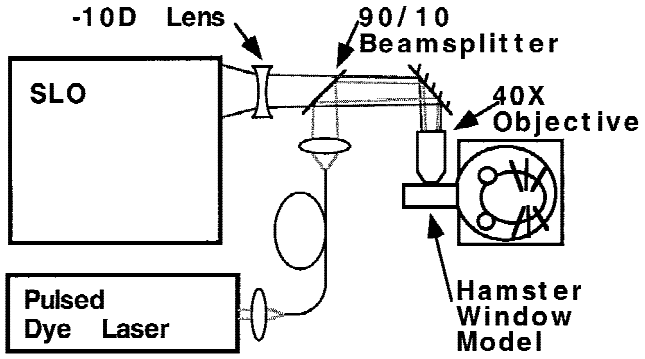

Fig. 1. Block diagram of the imaging and irradiation system. The hamster skin flap window preparation was imaged with a scanning laser ophthalmoscope augmented with external optics and irradiated with a pulsed dye laser operating at 577-nm, 2-μs pulse duration.

was maintained. Procedures were performed in accordance with a protocol approved by the University of Texas at Austin Institutional Animal Care and Use Committee. During surgical implantation and imaging/irradiation, the hamsters were anesthetized with xylazine and ketamine (3:4 ratio, 0.1 ml/100 g).

The blood vessels were imaged from the window side of the preparation. A scanning laser ophthalmoscope (Rodenstock SLO 101, Danbury, CT) operating at 30 frames per second was modified with external optics to provide a field of view of approximately 400 μm and a lateral resolution of 2 μm. Axial resolution was estimated to be better than 10 μm. The imaging source was a 632.8-nm helium:neon laser with a maximum power of approximately 400 μW at the tissue. Light from the therapeutic source, a flashlamp pumped dye laser (Candela LFDL-8, Wayland, MA), was inserted with a beamsplitter. The dye was rhodamine 575 in ethanol, and the laser was tuned to 577 nm. The pulse duration was 2 μs, as measured with a photodetector (EG&G Lite-Mike model 560b, Wellesley, MA). The laser beam profile was approximately Gaussian in shape, with a $1/e^2$ diameter of 300 μm, as measured by the knife-edge technique [10]. An overall block diagram of the imaging/irradiation system is shown in Figure 1, and a diagram of the hamster preparation in cross section is shown in Figure 2.

Capillaries and small arterioles/venules ranging from 10 to 120 μm in diameter were located with the confocal imaging system. Peak radiant exposure values of 0.1–5.0 J/cm^2 were used for irradiation of the blood vessels, as measured with a calibrated energy meter (Molectron Inc., Portland, OR). Either a single pulse or a sequence

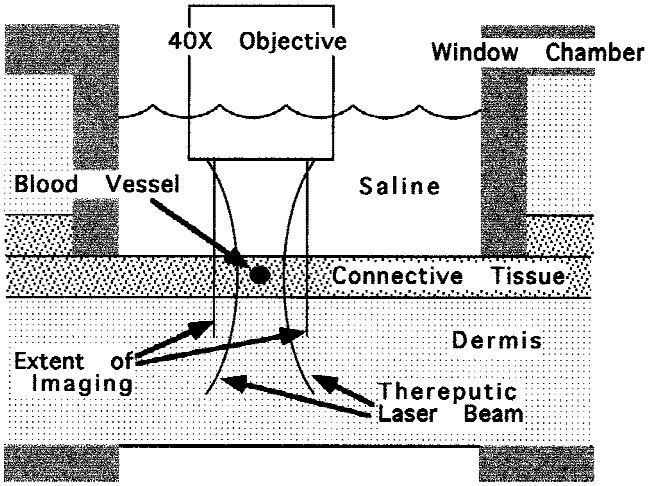

Fig. 2. Cross section diagram of the hamster skin flap window preparation, showing irradiated and imaged regions.

of 10 pulses at 10 Hz was applied. Damage was compiled into three categories: embolized or partly occluding coagula (category I), coagula causing complete blood flow stoppage (category II), or hemorrhage (category III). Blood vessels were irradiated more than once only if no change in morphology or blood flow rate was caused by the previous laser pulse. Approximately 240 irradiations were performed. All irradiated blood vessels were observed for a minimum of 5 min to ensure that damage was correctly categorized. Blood vessels with diameters of 61–120 μm, which could easily be located, were observed for patency at 24 hr from the time of irradiation.

For analysis purposes, blood vessels were divided into three ranges according to average diameter: 10–30, 31–60, and 61–120 μm. Probit analysis, assuming a sigmoid (integral of the Gaussian) probability distribution, was performed to determine the radiant exposure that would produce a 50% probability ("threshold") of causing the damage categories described above for 1 pulse and 10 pulses. Irradiations that caused higher categories of damage (such as hemorrhage) were not included in the probit analysis for lower categories of damage (such as embolized or partly occluding coagulum). Student's *t*-test was employed to assess the statistical significance of differences in the radiant exposure thresholds. Because of the small diameter of the irradiated blood vessels, no distinction was made between arterioles and venules.

The response of the blood vessels to the experimentally determined threshold radiant exposures was predicted by using a numerical model that combines optical and thermal components [11]. Due to the combined geometries of the beam profile and simulated blood vessel, a three-dimensional formulation and grid system were employed. The model was verified independently by using published analytical and numerical solutions.

The optical component incorporated a three-dimensional, nonhomogeneous-property Monte Carlo program. The tissue geometry was specified with a three-dimensional material grid that consisted of a large number of small voxels labeled by tissue type. The optical component solved for the distribution of absorbed energy, thus providing the heat source term for the thermal component. The three-dimensional thermal analysis employed an explicit finite difference (forward difference) technique to solve numerically the time-dependent Fourier heat conduction equation:

$$\frac{\partial^2 T}{\partial x^2}+\frac{\partial^2 T}{\partial y^2}+\frac{\partial^2 T}{\partial z^2}+\frac{S}{k}=\frac{1}{\alpha}\frac{\partial T}{\partial t} \qquad \text{where } \alpha=\frac{k}{\rho c} \tag{1}$$

and T (°C) is temperature, t (seconds) is time, S (W/m^3) is the heat source term, α (m^2/s) is thermal diffusivity, k (W/m-°C) is thermal conductivity, ρ (kg/m^3) is density, and c (J/kg-°C) is heat capacity [12]. Adiabatic boundary conditions were applied to the five internal tissue boundaries, whereas a convection condition was used on the superficial surface.

Thermal damage was computed based on the Arrhenius relation:

$$\Omega(t)=A\int_0^t \exp[-E_a/RT(\tau)]d\tau \tag{2}$$

where Ω is the coefficient of thermal damage, A (1/s) is the molecular collision rate, E_a (J/mol) is activation energy, and R is the universal gas constant (8.314 J/mol-°K). The distribution of thermal damage was updated each time step by using numerical integration of the Arrhenius relation by the trapezoidal rule. Because a clear set of Arrhenius coefficients for vessels or blood is not available, the damage computed with this relationship is relative.

The first step toward simulating laser–tissue interaction involved generating material grids for two relatively simple geometries, each consisting of a single, homogeneous, cylindrical blood vessel 30 or 60 μm in diameter embedded in a homoge-

TABLE 1. Optical Properties Used In Monte Carlo Modeling [14]

	$\mu_a(cm^{-1})$	$\mu_s(cm^{-1})$	g	n
Blood	354	468	0.995	1.33
Skin	1.5	156	0.787	1.37
Air	0	0	0	1.0

TABLE 2. Thermal Properties Used in Finite Difference Modeling [12,15]

k	0.5 (W/m–°C)
α	1.1×10^{-7} ($m^{2/s}$)
h	100 (W/m^2–°C)
A	3.1×10^{98} (1/s)
E_a	6.27×10^5 (J/mole)

neous layer of skin. A material grid consisting of 140 × 140 × 100 cube-shaped voxels measuring 5 μm on each side (length × width × depth) was used. The vessel was centered at a depth of 95 or 130 μm for simulations involving the 30- or 60-μm-diameter vessel, respectively.

Analysis was performed for each geometry by using a Gaussian laser beam with a $1/e^2$ diameter of 300 μm and optical properties corresponding to a wavelength of 577 nm. The thermal simulation involved a 2-μs heating period in which the source term (as calculated above) was applied, and the time step was 0.1 μs. A 1.0-s cooling phase was also simulated. Absorption and reduced scattering coefficients of bloodless hamster skin were obtained by measuring transmission and reflection in a spectrophotometer and by using the inverse adding-doubling program [13]. Published anisotropy and index of refraction values of human dermis were used as an estimate of hamster skin [14]. The optical properties of blood and thermal properties (uniform for blood and skin) used in the simulations were chosen from the literature [12,14,15]. Optical and thermal properties are listed in Tables 1 and 2, respectively.

RESULTS

Flowing blood was easily visualized in capillaries and small arterioles and venules with the confocal system. The highly reflective red blood cells were visible as moving bright dots, whereas the vessel wall was relatively dark. The collagen fibrils of the connective tissue were also visible as moderately bright strands. In the case of the smallest capillaries, single red blood cells could be seen traveling though the vessel. Laser coagulation of blood was immediately noticeable as an extremely bright aggregation of red blood cells. The depth discrimination of the system was sufficiently strong such that red blood cells moving near the superficial vessel wall could be distinguished from cells flowing at central or deep levels in the vessel. Figure 3A,B shows confocal images of a 45-μm-diameter blood vessel before and after, respectively, a laser pulse that caused an embolized coagulum. In Figure 3B, the coagulum is being carried downstream with the flow of blood.

The results of probit analysis to find the threshold radiant exposures for the previously described damage categories are summarized in Figure 4. There were insufficient data points (n = 28) in the 61–120-μm-diameter range to perform probit analyses, thus general observations are reported. From Figure 4 it can be seen that the threshold radiant exposures were greater for higher damage categories. In each damage category, the threshold radiant exposure was also greater for the larger blood vessel diameter range. In five of six instances, the thresholds when using 10 pulses at 10 Hz were lower than when using a single pulse. However, an analysis of the data indicated that not all trends were statistically significant ($P > 0.99$) because there was wide variation in radiant exposures required to achieve a category of damage, especially category III (hemorrhage).

A summary of statistical significance is given in Tables 3 and 4. For 10–30-μm-diameter blood vessels, there was a statistically significant difference in the threshold energies for each damage category. However, for 31–60-μm-diameter blood vessels, there was no statistically significant difference between the threshold for category II (coagula causing complete blood flow stoppage) and category III. For blood vessels with diameters greater than 60 μm, category II damage appeared unattainable. Only category I (embolized or partially occluding coagula) or III damage occurred. All blood vessels with diameters greater than 60 μm were patent at 24 hr regardless of the category of damage inflicted. There was a statistically significant increase in the threshold radiant exposure required to cause category II but not category I or III damage as the blood vessel diameter was increased from 10–30 μm to 31–60 μm. There was not a significant difference in the threshold radiant exposure required for any level of damage between a single pulse or 10 pulses at 10 Hz.

Figure 5A,B shows photographs of a window

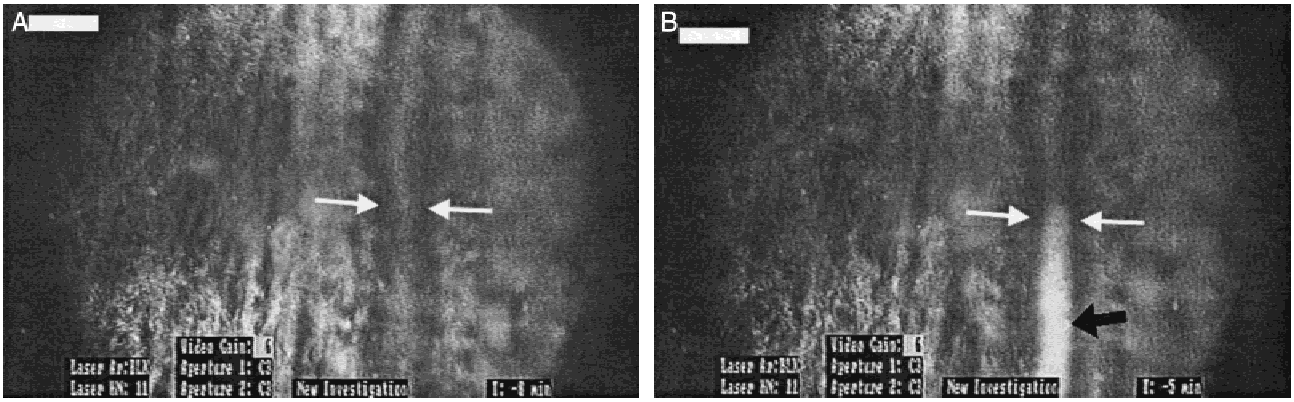

Fig. 3. Confocal images of a 45-μm-diameter blood vessel before (**A**) and after (**B**) a laser pulse that caused an embolized coagulum. Laser parameters: 577 nm, 2 μs, 2.8 J/cm^2, 300-μm-diameter Gaussian beam. White arrows indicate blood vessel diameter and the center of the laser beam. B: The bright mass (black arrow) is a coagulum traveling downstream with the flow of blood. Scale bar = 50 μm.

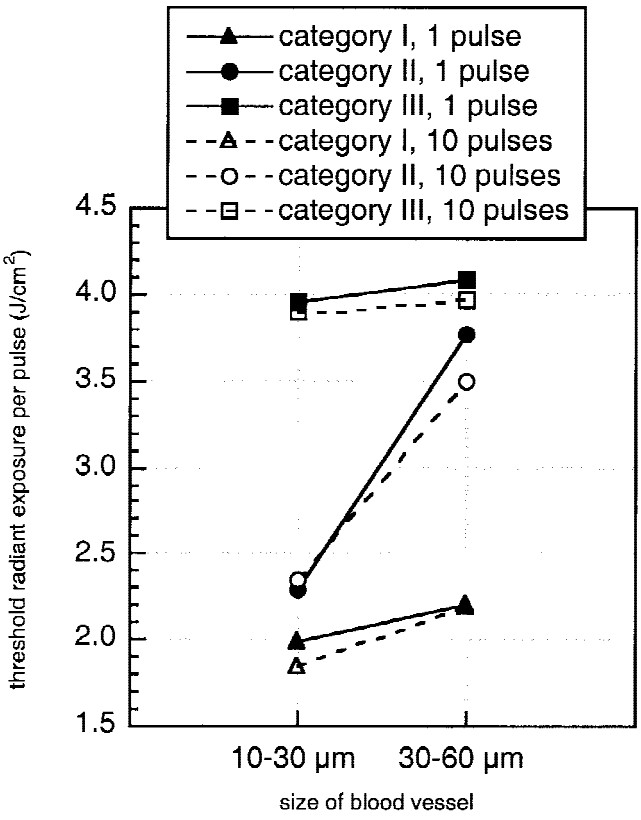

Fig. 4. Threshold radiant exposures required to inflict damage on blood vessels of two diameter ranges. Damage categories are defined as follows: I, embolized or partially occluding coagula; II, coagula causing complete blood flow stoppage; III, hemorrhage. Thresholds are 50% probability levels as determined by probit analysis.

TABLE 3. Differences Between Damage Categories Within a Blood Vessel Diameter Range*

	Damage category		
Range	I vs. II	I vs. III	II vs. III
10–30 μm	y	y	y
31–60 μm	y	y	n

* Statistically significant differences in radiant exposure threshold were determined with Student's t-test. y, significant at $P > 0.99$; n, not significant.

TABLE 4. Differences Between Blood Vessel Ranges Within a Damage Category*

Damage category	Range[a]
I	n
II	y
III	n

* Statistically significant differences in radiant exposure threshold were determined with Student's t-test. y, significant at $P > 0.99$; n, not significant.
[a] Range: 10–30 versus 31–60 μm diameter.

preparation before and immediately after irradiation, respectively. Irradiated small capillaries are not visible in this photograph. The arrow in Figure 5B shows the location of hemorrhage in a 40-μm-diameter blood vessel. The underlying blood vessels sustained no damage. This vessel healed at 24 hr and appeared to have normal blood flow.

Evidence of uneven damage was seen in blood vessels more than 30 μm in diameter. In every instance of a partly occluding coagulum, it was affixed to the superficial vessel wall. By adjusting the focus of the confocal microscope, blood could be seen flowing freely through the vessel deep to the coagulum. Rupture points leading to hemorrhage also occurred only at the superficial vessel wall.

The results of numerical modeling incorporating a 60-μm-diameter vessel is shown in Fig-

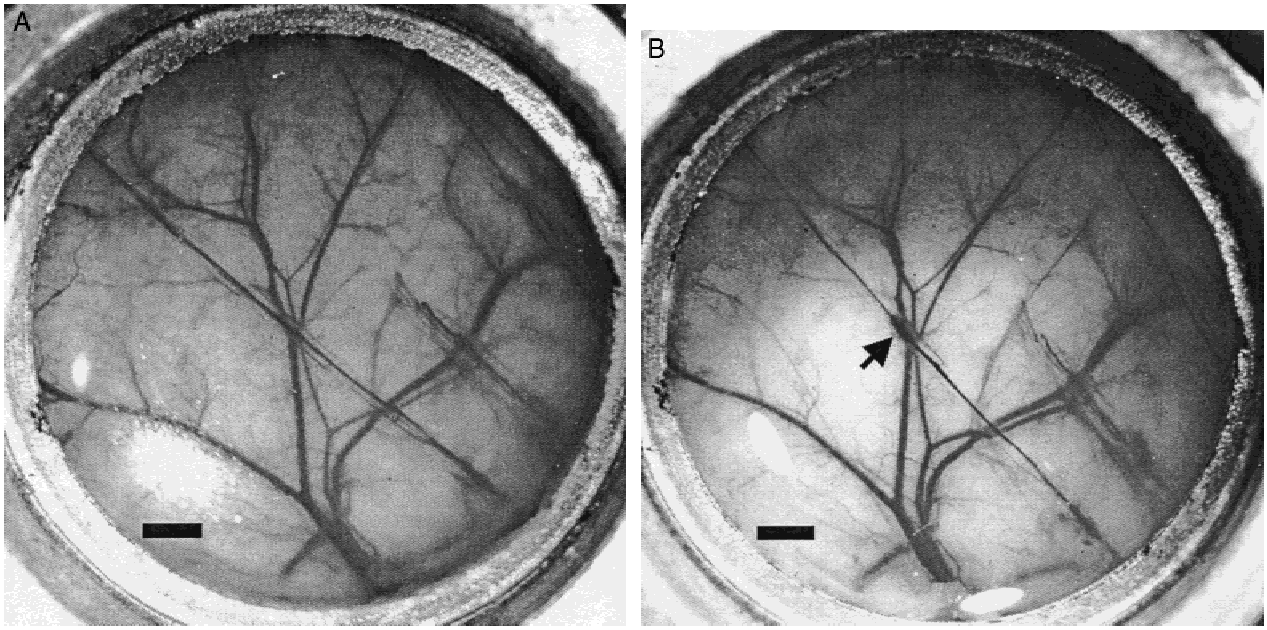

Fig. 5. Photographs of a window preparation before (**A**) and after (**B**) a laser pulse that caused hemorrhage in a 40-μm-diameter blood vessel (arrow in B). The underlying blood vessels were undamaged, and the blood vessel was healed at 24 hr. Laser parameters: 577 nm, 2 μs, 4.7 J/cm^2, 300-μm-diameter Gaussian beam. Scale bar = 1 mm.

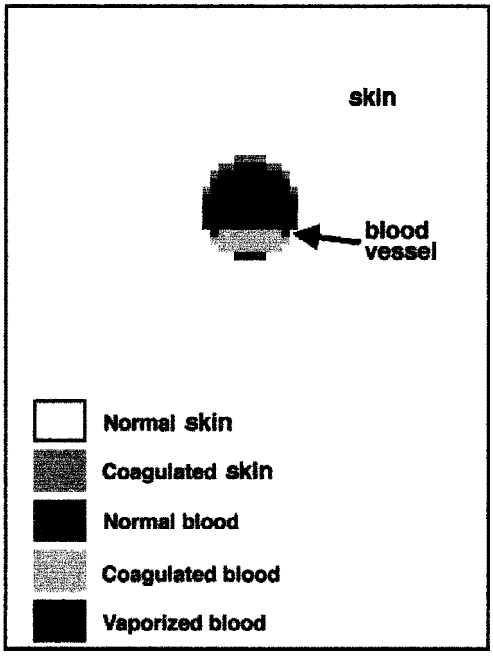

Fig. 6. Damage predicted by optical–thermal numerical modeling of a 60-μm-diameter vessel at the threshold radiant exposure for category II damage with a single pulse. Shadings represent different damage levels in the blood vessel and skin.

ure 6. The modeled radiant exposure was set to the threshold for category II damage with a single pulse. Damage is shown in a tissue cross section at the center of the beam. The major portion of the skin shows no damage except for a small layer of thermal damage limited to a 10-μm zone near the superficial wall of the vessel. The vessel itself shows three regions of damage. The superficial region of the blood vessel has a peak temperature above 100°C. The middle region of the vessel shows coagulation ($\Omega > 1$) but at temperatures below 100°C. The deepest region remains uncoagulated ($\Omega < 1$).

For the 60-μm-diameter vessel at the category III threshold, the skin appears undamaged except for the thin layer above the superficial vessel wall. Approximately two-thirds of the blood reached temperatures above 100°C. With the 30-μm-diameter vessel, almost the entire blood volume reached temperatures above 100°C at the category II threshold.

DISCUSSION

In general, to achieve maximum blood and vessel wall coagulation with a minimum of damage to the surrounding tissues, the laser pulse duration should be similar to the thermal relaxation time of the vessel, $t_r = d^2/16\alpha$, where d is the diameter of the vessel and α is the thermal diffusivity [1]. The pulse duration of the laser used in this study was much closer to the thermal relaxation time of the smallest blood vessels (48 μs) than that of the largest (6.9 ms), which may

explain the significant difference in the threshold radiant exposures for category II and III damage only for the smallest blood vessel diameter range. Because of the exponential decrease in laser fluence with depth in tissue, the radiant exposure needed to cause coagulation at deeper levels may cause hemorrhage even in small-diameter vessels at superficial levels. Because the energy deposition necessary to cause superficial coagulation or vaporization of blood is independent of the volume irradiated, it is not surprising that there was no significant difference in the threshold radiant exposure required to cause category I or II damage between the 10–30- and 31–60-μm blood vessel diameter ranges.

Previous Monte Carlo modeling [16] has determined the threshold radiant exposure for destruction of a single blood vessel at a dermal depth of 250 μm when using a laser wavelength of 585 nm. With a pulse duration of 450 μs, twice as much energy was required to destroy a 10-μm as opposed to a 60-μm-diameter vessel. When a pulse duration of 1.8 ms was used, the required increase was fourfold. Thus, PWSs consisting of many small blood vessels may be best treated with a laser of shorter pulse duration than commonly used. Although 2-μs pulses appear to be too short for clinical use [4], we were able to coagulate selectively very small vessels, and our results strengthen the idea that blood vessels of different diameters can be selectively destroyed by the appropriate combination of laser pulse duration and radiant exposure.

We found no statistically significant difference between one and 10 pulses (at 10 Hz), unlike Kimel et al. [17] who found an increasing probability of damage as the number of pulses was increased from one to three during a study of chick chorioallantoic membrane vessels. This variance may be due to the difference in vessel response to the pulse duration or wavelength used (2 μs and 577 nm in the present study vs. 450 μs or 10 ms and 585 nm in the study by Kimel et al.). Physiologic blood flow rate in hamster window blood vessels is 1–10 mm/s [9]. Therefore, the volume of blood heated by a subthreshold laser pulse may have flowed beyond the extent of the laser beam before the subsequent pulse was applied, thus preventing the superposition of damage.

Our results also demonstrate a potential shortcoming of 577 nm of radiation, the relatively short effective penetration depth in blood ($\delta' = 1/\mu_{t'} \sim 1/\mu_a \sim 30$ μm). Only the smallest vessels (10–30 μm in diameter) were heated throughout the blood volume. For larger vessels (>30 μm in diameter), the top 30 μm of blood shielded the remainder of the vessel from laser energy. The resultant uneven heating of blood was demonstrated by the partly occluding coagula affixed to the superficial vessel wall. Our results are in agreement with PWS histology data from Tan et al. [5] that showed aggregates of red blood cells at the superficial lumen of blood vessels treated with 577-nm pulsed dye irradiation. In the larger diameter blood vessels, we were able to confirm that blood vessels recovered from this localized damage.

The simulations at threshold for blood flow stoppage and hemorrhage in the 60-μm vessel predicted damage similar to that seen in the experiments. The finding that the superficial region of the blood vessel had temperatures above 100°C while the damage in deepest region remained minimal may explain why blood vessels greater than 60 μm in diameter could not be completely coagulated. Vaporization and rupture of the blood vessel may have occurred before a heat deposition was reached which could coagulate the deep region. The simulation also correctly suggested that partly occluding coagula appear at the superficial vessel wall. The simulation of the 30-μm-diameter vessel predicted temperatures above 100°C throughout most of the vessel at the experimentally determined threshold for coagulation. However, at this radiant exposure, hemorrhage rarely occurred. Previous studies have shown that temperatures above 100°C are required to vaporize soft tissue in air [18]. Superheating is believed to occur in laser–tissue interaction processes due to high rates of heat deposition. The latent heat of vaporization is also not included in these simulations. Also, blood vessel walls may expand to accommodate the increased pressure of a small amount of vaporization. Therefore, temperature must be used only as a warning of possible vaporization that may lead to hemorrhage.

The importance of vessel diameter must be included in any analysis of the treatment of PWSs or other procedures involving laser irradiation of blood vessels. For example, these data are applicable to retinal vessels. We expect that the diameter dependence seen in the present study for 2-μs pulses at 577 nm would occur for any pulse duration and wavelength. However, as pulse duration increases and/or the blood absorption coefficient decreases, there is a greater likelihood of uniform

heating of vessels in the range of 31–120 μm in diameter.

This study demonstrates that microsecond 577-nm dye laser pulses can predictably cause category I, II, or III damage in small (≤30 μm in diameter) blood vessels, but that permanent damage may not be achieved in larger vessels. Because many PWS vessels are >60 μm in diameter, these results provide insight into the failure of microsecond-pulse dye lasers to treat many stains effectively. The study also illustrates the effect of the strong absorption of 577-nm radiation in blood, which can cause partly occluding coagula to form on the superficial vessel wall while blood flows freely at deeper levels. Monte Carlo and finite difference numerical simulations were performed to analyze and evaluate the experimental results further. They show the ability of numerical models to simulate the irradiation of blood vessels in vivo but also show the limitations of applying arbitrary conditions for the prediction of complete processes such as blood vaporization and blood vessel hemorrhage. A clear criterion for coagulation of blood vessels is also essential for modeling the effect of laser parameters. These results are directly applicable to retinal blood vessel irradiation and indicate that vessel diameter should be considered when making predictions of intentional or accidental pulsed dye laser tissue damage.

ACKNOWLEDGMENT

A.J. Welch is the Marion E. Forsman Professor of Electrical and Computer Engineering.

REFERENCES

1. Anderson RR, Parrish JA. Microvasculature can be selectively damaged using dye lasers: a basic theory and experimental evidence in human skin. Lasers Surg Med 1981;1:263–276.
2. Nakagawa H, Tan OT, Parrish JA. Ultrastructure changes in human skin after exposure to a pulsed laser. J Invest Dermatol 1985;84:396–400.
3. Garden JM, Tan OT, Kerschmann R, Boll J, Furumoto H, Anderson RR, Parrish JA. Effect of dye laser pulse duration on selective cutaneous vascular injury. J Invest Dermatol 1986;87:653–657.
4. Hulsbergen Henning JP, van Gemert MJC, Lahaye CTW. Clinical and histological evaluation of portwine stain treatment with a microsecond-pulsed dye-laser at 577 nm. Lasers Surg Med 1984;4:375–380.
5. Tan OT, Morrison P, Kurban AK. 585 nm for the treatment of port-wine stains. Plast Reconstr Surg 1990;86: 1112–1117.
6. Pickering JW, van Gemert MJC. 585 nm for the laser treatment of port wine stains: a possible mechanism. Lasers Surg Med 1991;11:616–618.
7. van Gemert MJC, Welch AJ, Pickering JW, Tan OT, Gijsbers GHM. Wavelengths for laser treatment of port wine stains and telangiectasia. Lasers Surg Med 1995; 16:147–155.
8. Smithies DJ, Butler PH. Modelling the distribution of laser light in port-wine stains with the Monte Carlo method. Phys Med Biol 1995;40:701–731.
9. Gourgouliatos ZF, Welch AJ, Diller KR. Microscopic instrumentation and analysis of laser-tissue interaction in a skin flap model. J Biomech Eng 1991;113:301–307.
10. Khosrofian JM, Garetz BA. Measurement of a Gaussian laser beam diameter through the direct inversion of knife-edge data. Appl Optics 1983;22:3406–3410.
11. Pfefer TJ, Barton JK, Smithies DJ, Milner TE, Nelson JS, van Gemert MJC, Welch AJ. Laser treatment of port wine stains: three-dimensional simulation using biopsy-defined geometry in an optical–thermal model. Proc SPIE 1998;3245:322–333.
12. Orr LS, Eberhart RC. Overview of bioheat transfer. In: Welch AJ, van Gemert MJC, eds. Optical–thermal response of laser-irradiated tissue. New York: Plenum Press; 1995. p 367–384.
13. Prahl SA, van Gemert MJC, Welch AJ. Determining the optical properties of turbid media using the adding-doubling method. Appl Optics 1993;32:559–568.
14. van Gemert MJC, Welch AJ, Pickering JW, Tan OT. Laser treatment of port wine stains. In: Welch AJ, van Gemert MJC, eds. Optical–thermal response of laser-irradiated tissue. New York: Plenum Press; 1995. p 789–830.
15. Henriques FC, Moritz AR. Studies in thermal injury V: the predictability and significance of thermally induced rate processes leading to irreversible epidermal injury. Arch Pathol 1947;43:489–502.
16. de Boer JF, Lucassen GW, Verkruysse W, van Gemert MJC. Thermolysis of port-wine-stain blood vessels: diameter of a damaged blood vessel depends on the laser pulse length. Lasers Med Sci 1996;11:177–180.
17. Kimel S, Svaasand LO, Hammer-Wilson M, Schell MJ, Milner TE, Nelson JS, Berns MW. Differential vascular response to laser photothermolysis. J Invest Dermatol 1994;103:693–708.
18. Torres JH, Motamedi M, Welch AJ. Disparate absorption of argon laser radiation by fibrous versus fatty plaque: implications for laser angioplasty. Lasers Surg Med 1990;10:149–157.